Theor Chem Acc (1998) 99:384–390
DOI 10.1007/s002149800m31

Theoretical Chemistry Accounts

Regular article

Calculation of macroscopic first- and third-order optical susceptibilities for the benzene crystal

H. Reis[1], S. Raptis[1], M.G. Papadopoulos[1], R.H.C. Janssen[2], D.N. Theodorou[2], R.W. Munn[3]

[1] Institute of Organic and Pharmaceutical Chemistry, National Hellenic Research Foundation, Vasileos Constantinou 48, GR-11635 Athens, Greece
[2] Department of Chemical Engineering, University of Patras and Institute of Chemical Engineering and High Temperature Chemical Processes, GR-26500 Patras, Greece
[3] Department of Chemistry, UMIST, Manchester M60 1QD, UK

Received: 11 February 1998 / Accepted: 6 July 1998 / Published online: 18 September 1998

Abstract. Starting from a set of high-level ab initio frequency-dependent molecular first- and third-order polarizabilities, the macroscopic first-order (linear) and third-order (cubic) susceptibilities of the benzene crystal are calculated. Environmental effects are taken into account using a rigorous local-field theory and are compared with the anisotropic Lorentz field factor approach. The experimentally determined first-order susceptibility of crystalline benzene is accurately reproduced. Dispersion curves for the first-order susceptibility and results for electric-field-induced second-harmonic generation and third-harmonic generation experiments are predicted. Comparison with similar calculations conducted in the course of molecular simulations of liquid benzene shows that the theoretical results for the two phases are of comparable accuracy. Overall, the results show that for the fairly compact nonpolar benzene molecules, environmental effects on the effective molecular response are small.

Key words: Susceptibilities – Benzene crystal – Polarizabilities – Hyperpolarizabilities

1 Introduction

Optical linear and nonlinear susceptibilities are usually measured in condensed matter, where the underlying molecular properties are strongly affected by the influence of the environment and are therefore not directly comparable with the results of theoretical calculations which yield the linear and nonlinear polarizabilities of the isolated molecule. Recently, a molecular dynamics calculation of the macroscopic first- and third-order susceptibilities of liquid benzene has been published, starting from molecular high-level ab initio polarizabilities and hyperpolarizabilities [1]. The results of that purely computational work showed good agreement with available experimental data. The question then arises whether a similar approach can be applied equally successfully to crystals.

A method for the calculation of crystal susceptibilities from molecular properties has been derived by Munn and coworkers [2, 3]. In this model the local fields experienced by the molecules in the crystal are rigorously calculated employing the point-dipole approximation by summing the fields arising from the surrounding dipoles in the crystal. This contrasts with the less rigorous but often used Lorentz field factor approach, which is an anisotropic extension of the local-field factor calculated by Lorentz for cubic and isotropic media.

The results of the application of the two approaches to crystalline benzene are reported in this work and compared with the results for liquid benzene.

An essential aim of this project is the complete description of the nonlinear optical (nlo) properties, i.e. the calculation of both the molecular polarizability and hyperpolarizabilities and the macroscopic susceptibilities, in the liquid and solid state using the appropriate computational techniques. This goal may help us to clarify open questions related to the effect of environmental interactions on the nlo properties.

2 Theory

The theory of nonlinear response of molecular crystals in the framework of local-field theory has been described at length [2, 5]. Only a short summary of the parts relevant for the case under consideration is given here.

Let a molecular crystal contain Z identical molecules labelled k per unit cell. If the crystal is subjected to an

Correspondence to: M.G. Papadopoulos
e-mail: mpapad@eie.gr

external electric field, the induced dipole moment $\underline{p}_k$ of a molecule is

$$\underline{p}_k = \underline{\underline{\alpha}}_k \cdot \underline{F}_k + \underline{\underline{\underline{\beta}}}_k : \underline{F}_k\underline{F}_k + \underline{\underline{\underline{\underline{\gamma}}}}_k \vdots \underline{F}_k\underline{F}_k\underline{F}_k + \dots \ , \tag{1}$$

where for brevity we do not indicate any frequency dependence. The quantities $\underline{\underline{\alpha}}_k$, $\underline{\underline{\underline{\beta}}}_k$, $\underline{\underline{\underline{\underline{\gamma}}}}_k$ are the molecular polarizability and the first and second hyperpolarizabilities, respectively. Considering only dipole–dipole interactions, the effective polarizability and hyperpolarizabilities in the crystal coincide with the properties of the free molecules for nonpolar molecules like benzene. $\underline{F}_k$ is the local electric field acting on the molecule and is the sum of the macroscopic electric field $\underline{E}$ and the field due to the induced dipole moments of the surrounding molecules in the crystal. It can be written as

$$\underline{F}_k = \underline{E} + \sum_{k'} \underline{\underline{L}}_{kk'} \cdot \underline{p}_{k'} (\epsilon_0 v)^{-1} \ , \tag{2}$$

where v denotes the volume of the unit cell, ϵ_0 is the permittivity of free space (=8.8542 × 10^{-12} V $C^{-1}m^{-1}$) and $\underline{\underline{L}}_{kk'}$ is the Lorentz-factor tensor [4].

The macroscopic polarization $\underline{P}$ of the crystal induced by the external field $\underline{E}$ can similarly be written as a series in $\underline{E}$

$$\underline{P}/\epsilon_0 = \underline{\underline{\chi}}^{(1)} \cdot \underline{E} + \underline{\underline{\underline{\chi}}}^{(2)} : \underline{EE} + \underline{\underline{\underline{\underline{\chi}}}}^{(3)} \vdots \underline{EEE} + \dots \ , \tag{3}$$

where $\chi^{(n)}$ are the macroscopic electric n-th order susceptibilities. The molecular induced dipole moment and the macroscopic polarization $\underline{P}$ of the crystal are related via

$$\underline{P} = \sum_k \underline{p}_k v^{-1} \ . \tag{4}$$

As shown by Hurst and Munn [2], algebraic manipulation of Eqs. (1)–(4) leads to the desired connection between the macroscopic susceptibilities and the molecular polarizability and hyperpolarizabilities. For a centrosymmetric molecule like benzene with a first hyperpolarizability $\underline{\underline{\underline{\beta}}}$ that vanishes by symmetry, the equations reduce to

$$\underline{\underline{\chi}}^{(1)}(-\omega_0;\omega_0) = (\epsilon_0 v)^{-1} \sum_k \underline{\underline{\alpha}}_k(-\omega_0;\omega_0) \cdot \underline{\underline{d}}_k(\omega_0) \ , \tag{5}$$

$$\underline{\underline{\underline{\chi}}}^{(2)}(-\omega_0;\omega_1,\omega_2) = 0 \ , \tag{6}$$

$$\underline{\underline{\underline{\underline{\chi}}}}^{(3)}(-\omega_0;\omega_1,\omega_2,\omega_3) = (\epsilon_0 v)^{-1} \sum_k \underline{\underline{\underline{\underline{\gamma}}}}_k(-\omega_0;\omega_1,\omega_2,\omega_3) \vdots [\underline{\underline{d}}_k(\omega_3)\underline{\underline{d}}_k(\omega_2)\underline{\underline{d}}_k(\omega_1)\underline{\underline{d}}_k(\omega_0)] \ , \tag{7}$$

Here the frequency dependence has been considered explicitly, and the output frequency ω_0 is the sum of the input frequencies. The contraction between $\underline{\underline{\underline{\underline{\gamma}}}}_k$ and the quantity in square brackets in Eq. (7) is to be understood as $[\underline{\underline{\underline{\underline{\gamma}}}} \vdots (\underline{dddd})]_{mnop} = \sum_{ijkl} \gamma_{ijkl} d_{lp} d_{ko} d_{jn} d_{im}$. The local-field tensors $\underline{\underline{d}}_k$ are given by

$$\underline{\underline{d}}_k = \sum_{k'} \underline{\underline{D}}_{kk'} = \sum_{k'} \left[\underline{\underline{\mathbf{I}}} - \underline{\underline{\mathbf{L}}} \cdot \underline{\underline{\boldsymbol{\alpha}}}/(\epsilon_0 v)\right]^{-1}_{kk'} \ . \tag{8}$$

The boldfaced matrices are of order $3Z \times 3Z$: $\underline{\underline{\mathbf{I}}}$ is the generalized unit matrix of order $3Z$ with submatrices $\underline{\underline{I}}_{kk'} = \underline{\underline{1}}\delta_{kk'}$, where $\underline{\underline{1}}$ is the 3 × 3 unit matrix, while $\underline{\underline{\mathbf{L}}}$ and $\underline{\underline{\boldsymbol{\alpha}}}$ have submatrices $\underline{\underline{L}}_{kk'}$ and $\underline{\underline{\alpha}}_k \delta_{kk'}$, respectively.

As stated above, the equations given assume the point-dipole approximation to be valid. It has been shown [5] that this approximation is not satisfactory for the calculation of $\underline{\underline{\alpha}}$ from $\underline{\underline{\chi}}^{(1)}$ in the case of some polyphenyls and condensed aromatic hydrocarbons such as biphenyl, naphthalene and their higher homologues. This problem has been ascribed to the fact that the point–dipole description does not take into account the finite size and shape of the charge density in the molecules, which gives rise to nonlocal susceptibility functions $\chi^{(n)}(\underline{r}, \underline{r}')$ [6]. This effect can be partly taken into account by considering each molecule as composed of several submolecules j each treated as a point dipole. Formally, only minor changes are then necessary in the equations given above, namely replacing the index k by the composite index kj. In the calculation of the Lorentz-factor tensors the contribution of different submolecules in the same molecule has to be excluded, so that one part of a molecule does not polarize another part of the same molecule.

Often the influence of the environment on the molecular properties in crystals is treated within the less rigorous oriented-gas model, together with the anisotropic Lorentz field factor approximation [7]. Here the local fields $\underline{\underline{d}}$ in Eqs. (5)–(7) are obtained from the refractive indices n_i by

$$d_{ij}(\omega) = \delta_{ij}[n_i(\omega)^2 + 2]/3 \ , \tag{9}$$

where i and j label the crystallographic axes a, b, c.

Although it is much easier to apply than the more rigorous approach, it has been shown that it may lead to wrong results, in particular giving the wrong anisotropy for elongated molecules [8].

3. Results and discussion

The static and frequency-dependent ab initio molecular polarizability and second hyperpolarizability components α_{ll} and γ_{lmno} are shown in Table 1. They were calculated at the MP4(SDQ) level (static) with the GAUSSIAN 94 software package [9] and at the coupled-perturbed Hartree–Fock (CPHF) level (static and frequency-dependent) with the GAMESS software package [10] using the polarization-consistent Sadlej basis set [11]. The HF values for α_{ll} agree with those given by Lazzeretti et. al [12] for the same basis set. Values for γ_{lmno} for smaller basis sets and lower level of correlation (MP2) have been given by Perrin et al. [13] and Adant et al. [14]. The input geometry used is the experimentally determined geometry of benzene in the gas phase [15] (C—C 0.13964 nm, C—H 0.10831 nm, symmetry D_{6h}). The differences from the geometry of benzene in the crystal [16] are smaller than the experimental uncertainties, indicating the rather weak effect of the intermolecular forces in the benzene crystal. The

Table 1 Static and frequency-dependent molecular polarizabilities (α_{ll} / 10^{-40} C^2 m^2 J^{-4}) and second hyperpolarizabilities (γ_{lmno} /10^{-64} C^4 m^4 J^{-3}) for third-harmonic generation [THG: $\gamma(-3\omega;\ \omega,\ \omega,\ \omega)$] and electric-field-induced second-harmonic generation [EFISH: $\gamma(-2\omega;\ \omega,\ \omega,\ 0)$] of benzene at MP4(SDQ) and coupled-perturbed Hartee–Fock (CPHF) levels

λ/nm	CPHF					MP4(SDQ)
	∞	1064		694.3		∞
α_{xx}	13.10	13.27		13.51		13.19
α_{zz}	7.503	7.568		7.688		7.376
		THG	EFISH	THG	EFISH	
γ_{xxxx}	1253	1707	1451	3019	1812	1510
γ_{zzzz}	1509	2118	1775	3867	2263	1357
γ_{xxyy}	418	569	483	1006	603	514
γ_{xxzz}	676	1039	831	2248	1119	621

molecular x and y axes lie in the plane of the molecule. Due to molecular symmetries, the components of $\underline{\underline{\alpha}}$ and $\underline{\underline{\underline{\gamma}}}$ are symmetrical in x and y, and therefore only the x components are given in Table 1. In the static case, Kleinman symmetry holds, i.e. permutations of the set of indices $(ijkl)$ do not change the value of γ_{ijkl}. This symmetry is broken if the external electric fields are time-dependent. However, for the frequency-dependent electric-field-induced second harmonic generation (EFISH) and third-harmonic generation (THG) calculations reported here, the deviations from Kleinman symmetry are less than 3% at a wavelength of $\lambda = 694.3$ nm and less than 1% at $\lambda = 1064$ nm. The corresponding components are therefore not given in Table 1.

Three models have been employed for the calculation of the macroscopic susceptibilities $\underline{\underline{\chi}}^{(1)}$ and $\underline{\underline{\underline{\chi}}}^{(3)}$ for the benzene crystal with the molecular polarizabilities of Table 1 as input data:

1. Rigorous local field theory (RLFT), as outlined in Sect. 2, approximating a molecule of benzene by a single point dipole situated at the centre of mass of the molecule. This model will be abbreviated as RLFT1.
2. A model abbreviated as RLFT6, which is the same as RLFT1 except that now each benzene molecule is treated as composed of six submolecules placed at the carbon atoms.
3. The anisotropic Lorentz field factor approximation (ALFFA), as given by Eqs. (5) and (7) with Eq. (9). Usually, the refractive indices in Eq. (9) are taken from experiment. However, as far as we are aware, the dispersion of the refractive indices for the benzene crystal has not been determined yet and values are available only for the single wavelength $\lambda = 546$ nm [17, 22]. Use of these values would introduce a certain amount of error whenever the wavelengths of interest differ from this value, i.e. in all cases considered except $\underline{\underline{\chi}}^{(1)}$ at $\lambda = 546$ nm. Therefore, we calculated the refractive indices by means of the anisotropic Lorenz-Lorentz formula [22, 24]

$$\frac{n_i^2 - 1}{n_i^2 + 2} = \frac{1}{3\epsilon_0 v} \sum_k (\alpha_{ii})_k \ , \tag{10}$$

where $(\alpha_{ii})_k$ is the ith diagonal component of $\underline{\underline{\alpha}}_k$ in the crystallographic coordinate system. For comparison, we also give the results for $\underline{\underline{\chi}}^{(1)}(\lambda = 546\ \text{nm})$ in Table 3 using the experimental refractive indices ($n_a = 1.544$, $n_b = 1.646$, $n_c = 1.550$). This variant of the anisotropic Lorentz field factor approximation is abbreviated as ALFFA/Emp.

The division of a molecule into submolecules in RLFT is rather arbitrary, being a poorly-defined compromise between the rigorous but numerically intractable nonlocal formulation of the molecular dipole moment in terms of charge densities [6] and the well-defined, tractable but less rigorous point-dipole model. By comparing the results of models (1) and (2), i.e. the point-dipole and the six-submolecule model, respectively, it should be possible to assess the importance of molecular extension in determining the crystal susceptibilities of benzene. Bounds and Munn [5] calculated the molecular polarizability of benzene from the experimental $\underline{\underline{\chi}}^{(1)}$ for comparison with more extended aromatic hydrocarbons, for which the point-dipole model evidently failed, and reported that the point-dipole model was sufficient for benzene, although no results were given for any other partitions. Hence it may also be interesting to see whether there is a similarly small effect on $\underline{\underline{\underline{\chi}}}^{(3)}$ of different schemes for dividing benzene into submolecules. As far as we know, this possibility has not previously been investigated.

The crystal structure of benzene (orthorhombic, space group *Pbca*, four molecules per unit cell) and the dimensions of the unit cell at $T = 270$ K $[(a, b, c) = (0.7460,\ 0.9666,\ 0.7034)$ nm] were taken from Ref. [16].

The results of the calculations of $\chi_{ii}^{(1)}$ and $\chi_{iijj}^{(3)}$ are given in the Tables 2–4. In Table 2 the results for $\chi_{ii}^{(1)}$ for static CPHF and MP4(SDQ) for the models RLFT1 and RLFT6 are shown. As the values for α_{xx} and α_{zz} in Table 1 show, the differences between the correlated and uncorrelated levels of theory are very small, indicating an essentially negligible influence of correlation on the polarizability $\underline{\underline{\alpha}}$ and consequently on $\underline{\underline{\chi}}^{(1)}$ of benzene. It is not possible at present to calculate the frequency dependence of the polarizability at the MP4 level. It has been shown in several cases, however, that the frequency dependence of the correlation effect calculated at the MP2 level can be accounted for or by a multiplicative correction [18–20], i.e.

$$\alpha_{ll}(\text{MP2}, \omega) = \frac{\alpha_{ll}(\text{SCF}, \omega)}{\alpha_{ll}(\text{SCF}, 0)} \alpha_{ll}(\text{MP2}, 0) \ , \tag{11}$$

Table 2. Calculated static first-order susceptibilities $\chi^{(1)}$ of the benzene crystal at CPHF and MP4(SDQ) levels

Static	$\chi_{aa}^{(1)}$	$\chi_{bb}^{(1)}$	$\chi_{cc}^{(1)}$
CPHF/RLFT1	1.390	1.649	1.409
CPHF/RLFT6	1.350	1.679	1.359
MP4(SDQ)/RLFT1	1.386	1.664	1.406
MP4(SDQ)/RLFT6	1.346	1.694	1.354

(and similarly for β_{lmn}, γ_{lmno}), or by an additive correction [21]

$$\alpha_{ll}(\mathrm{MP2},\omega) = [\alpha_{ll}(\mathrm{SCF},\omega) - \alpha_{ll}(\mathrm{SCF},0)] + \alpha_{ll}(\mathrm{MP2},0) \ , \quad (12)$$

provided that the frequencies are far removed from any electronic resonances. It has been argued that the same corrections should also be applicable to higher levels of correlation [18]. In the case of the MP4(SDQ) calculations for benzene considered here, both methods of correction would result in very small changes for the calculated first-order susceptibility. Thus we do not expect significant correlation effects on the frequency-dependent CPHF calculations for the first-order susceptibility reported here, at least outside the region of linear optical absorption.

In Table 3 we compare the experimental $\underline{\underline{\chi}}^{(1)}$, determined at $\lambda = 546$ nm [17, 22] with the results of the calculations with ab initio CPHF input values at the same wavelength for all the local-field models considered. All models show good agreement with the experimental values, as evidenced by the mean relative deviations given in column 4. All models give the right order of the components $\chi^{(1)}_{bb} > \chi^{(1)}_{cc} > \chi^{(1)}_{aa}$, but the ALFFA calculations considerably overestimate the anisotropy $\delta^{(1)}$ of $\underline{\underline{\chi}}^{(1)}$, defined by

$$\delta^{(1)} = \chi^{(1)}_{bb} - (\chi^{(1)}_{aa} + \chi^{(1)}_{cc})/2 \ . \quad (13)$$

In Fig. 1 the dispersion of the calculated $\chi^{(1)}_{ii}$ values is shown for $i = a$ and $i = b$, the component $\chi^{(1)}_{cc}$ being very similar to $\chi^{(1)}_{aa}$. The forms of the dispersion curves for the three models are very similar, but in magnitude the ALFFA model differs considerably from the other two models.

The results for $\chi^{(3)}_{iijj}$ for the static case and the two frequently used laser wavelengths $\lambda = 1064$ nm and $\lambda = 694.3$ nm are shown in Table 4. THG and EFISH are simulated.

The static values of γ_{llmm} change by 8–23% from the CPHF level to the MP4(SDQ) level (see Table 1). One may note especially the reversal of the magnitudes for the diagonal components: $\gamma_{xxxx} < \gamma_{zzzz}$ for CPHF, but $\gamma_{xxxx} > \gamma_{zzzz}$ for MP4. Although these changes are more pronounced than in the case of the linear polarizability α, they are by no means as dramatic as those which may result from including correlation, e.g. in urea the values calculated for γ (CPHF) increase by a factor of ~2.3 at the MP4 level [23]. The changes between CPHF and MP4 for γ manifest themselves in slightly smaller differences of the $\chi^{(3)}_{iijj}$ values of 3–18% , owing to the partial averaging effect of the different orientations of the four molecules in the unit cell. As in the case of $\underline{\underline{\chi}}^{(1)}$, the models RLFT1 and RLFT6 yield similar results, the components $\chi^{(3)}_{iijj}$ differing by up to 10% for the static case and for THG and EFISH at $\lambda = 1064$ nm and by up to ~13% for THG and EFISH at $\lambda = 694.3$ nm. The differences between ALFFA and the RLFT methods are

Table 3. Experimental [17] and calculated CPHF first-order susceptibilities $\chi^{(1)}_{ii}$ of the benzene crystal at $\lambda = 546$ nm; $\overline{\Delta}$ is the mean percentage deviation of the calculated from the experimental values, $\delta^{(1)}$ is the anisotropy defined in Eq. (13), the numbers in parentheses are the percentage deviation of the calculated values from the experimental value

	$\chi^{(1)}_{aa}$	$\chi^{(1)}_{bb}$	$\chi^{(1)}_{cc}$	$\overline{\Delta}$	$\delta^{(1)}$
ALFFA	1.404	2.002	1.474	7.9%	0.563 (78%)
ALFFA/Emp.	1.397	1.885	1.451	5.4%	0.461 (46%)
RLFT1	1.487	1.774	1.506	6.2%	0.278 (−12%)
RLFT6	1.441	1.808	1.448	4.4%	0.363 (15%)
Exp.	1.384	1.709	1.403		0.316

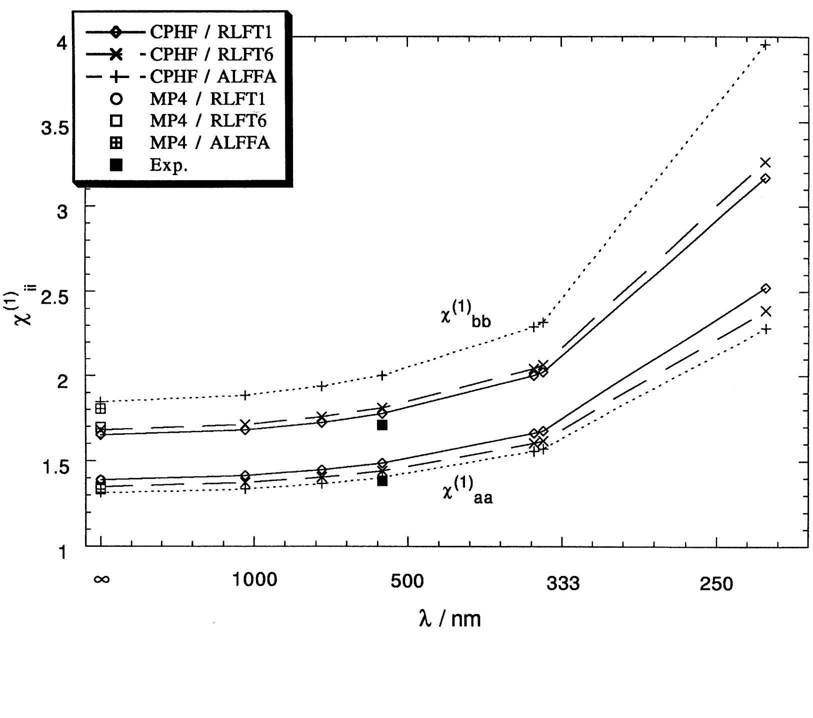

Fig. 1. Calculated dispersion curves for $\chi^{(1)}_{aa}$ and $\chi^{(1)}_{bb}$ for the benzene crystal

Table 4. Calculated third-order susceptibilities $\chi^{(3)}_{ijkl}/10^{-24}$ $(\mathrm{m/V})^2$ of the benzene crystal. Differences due to the violation of Kleinman symmetry do not exceed 3% for $\lambda = 694.3$ nm and 1% for $\lambda = 1064$ nm

	Static					
	CPHF			MP4(SDQ)		
	ALFFA	RLFT1	RLFT6	ALFFA	RLFT1	RLFT6
$\chi^{(3)}_{aaaa}$	653	807	735	628	778	704
$\chi^{(3)}_{bbbb}$	814	506	560	950	599	656
$\chi^{(3)}_{cccc}$	684	788	718	668	762	687
$\chi^{(3)}_{aabb}$	257	226	227	266	237	235
$\chi^{(3)}_{aacc}$	147	176	164	166	196	178
$\chi^{(3)}_{bbcc}$	260	222	224	273	235	233
	$\lambda = 1064$ nm (CPHF)					
	THG			EFISH		
$\chi^{(3)}_{aaaa}$	1028	1290	1165	807	1006	913
$\chi^{(3)}_{bbbb}$	1247	757	847	986	611	679
$\chi^{(3)}_{cccc}$	1081	1257	1137	847	981	891
$\chi^{(3)}_{aabb}$	397	356	356	314	279	280
$\chi^{(3)}_{aacc}$	200	245	227	169	206	191
$\chi^{(3)}_{bbcc}$	412	351	355	318	275	277
	$\lambda = 694.3$ nm					
$\chi^{(3)}_{aaaa}$	2494	3247	2867	1126	1416	1245
$\chi^{(3)}_{bbbb}$	3114	1698	1950	1356	818	891
$\chi^{(3)}_{cccc}$	2659	3145	2775	1184	1380	1215
$\chi^{(3)}_{aabb}$	964	892	876	432	385	375
$\chi^{(3)}_{aacc}$	346	435	396	204	251	227
$\chi^{(3)}_{bbcc}$	1095	868	886	445	381	374

more pronounced: up to 70% from the RLFT6 method and up to 80% from RLFT1. Even more interesting are the changes of the relative magnitudes of the components between the models. While for the cross terms $\chi^{(3)}_{aabb} \sim \chi^{(3)}_{bbcc} > \chi^{(3)}_{aacc}$ for all three models, for the diagonal terms $\chi^{(3)}_{aaaa} \geq \chi^{(3)}_{cccc} \gg \chi^{(3)}_{bbbb}$ for RLFT1 and RLFT6, but $\chi^{(3)}_{bbbb} \gg \chi^{(3)}_{cccc} \geq \chi^{(3)}_{aaaa}$ for ALFFA. Further, the difference between the largest and the smallest diagonal component, i.e. $\chi^{(3)}_{aaaa} - \chi^{(3)}_{bbbb}$ is smaller for RLFT6 than for RLFT1. Thus the RLFT6 model, which unlike the other models is designed to take some account of the size of the molecules, again gives results that lie between those given by the two other models.

It is unlikely that the small differences between the values of the components of $\underline{\underline{\underline{\chi}}}^{(3)}$ calculated by the RLFT1 and RLFT6 models can be resolved by any experimental measurement. On the other hand, the different orderings of the diagonal components predicted by ALFFA and RLFT1/RLFT6 should be observable experimentally. Therefore it should be possible to check the predictions of the two different theoretical models ALFFA and RLFT1/RLFT6, at least qualitatively.

Unfortunately, data on $\chi^{(3)}_{iijj}$ for crystalline benzene are very scarce in the literature. We are aware of only one experimental report by Hochstrasser et al. [17] on resonant four-wave mixing at $T = 2$ K. They give an estimate of the nonresonant component $\chi^{(3)}_{aaaa}(-\omega_0; \omega_1, \omega_1, -\omega_2)$ for $\lambda_1 = 2\pi c_0/\omega_1 \sim 510$ nm and $\lambda_2 = 2\pi c_0/\omega_2 = 603$ nm of 2.7×10^{-14} cm^2 erg^{-1}, which after conversion to SI units and multiplication by 4/3 (c.f. Ref. [25], Appendix D) yields 503×10^{-24} $(\mathrm{m/V})^2$. This value was considered quite a crude estimate by the authors themselves and so it is not surprising that it compares rather badly with the much higher values given in Table 4. The calculated values refer to $T = 270$ K and should further increase with decreasing temperature, considering the expected increase of the local-field factors with decreasing temperature caused by the thermal contraction of the crystal.

In order to compare the results given here with those of the computer simulation of the liquid [1], which yield isotropic results we define average values by

$$\langle \chi^1 \rangle = 1/3 \sum_i \chi^{(1)}_{ii} \quad , \tag{14}$$

$$\langle \chi^3 \rangle_d = 1/3 \sum_i \chi^{(1)}_{iiii} \quad , \tag{15}$$

$$\langle \chi^3 \rangle_c = 1/3 \sum_{ij} \chi^{(1)}_{iijj}(1 - \delta_{ij}) \quad . \tag{16}$$

The results for RLFT6 at the MP4(SDQ) level are $\langle\chi^1\rangle = 1.465$, $\langle\chi^3\rangle_d = 671 \times 10^{-24}$ (m/V)^2, $\langle\chi^3\rangle_c = 215 \times 10^{-24}$ (m/V)^2 and compare quite well with the corresponding values for the liquid calculated at the MP2 level: $\chi^1_{II} = 1.242$, $\chi^3_{IIII} = 533 \times 10^{-24}$ (m/V)^2, $\chi^3_{IIJJ} = 177 \times 10^{-24}$ (m/V)^2 (in the notation of Ref. [1], I and J denote two perpendicular axes in the laboratory frame). Owing to the higher density of the solid, the local fields and therefore also the mean susceptibilities of the crystals are higher than those of the liquid. In the case of the liquid, the calculated results compare favourably with the experimental EFISH measurements of Levine and Bethea [25]. This fact may also raise doubts about the reliability of the value estimated by Hochstrasser et al. for the nonresonant part of $\chi^{(3)}_{aaaa}$.

4 Synopsis and conclusions

Several applications of the rigorous local-field to various crystals have already appeared in the literature [26], using as input parameters semiempirical or low-level ab initio values with their inherent weaknesses, making it difficult to assess the performance of the local-field theory itself. To our knowledge, the present paper is the first report about an application using molecular polarizabilities calculated at a reasonably high ab initio level of computational chemistry and should therefore be less affected by the limitations of this part of the calculations.

We have shown that the calculation of the macroscopic crystal susceptibilities for benzene in the rigorous local-field theory yields reasonable results, which at least in the case of the first-order susceptibility compare favourably with experiment, while for the third-order susceptibility the comparison with the only available experimental datum is less encouraging. However, this value should be considered as an estimate and more accurate experimental data are required in order to make reliable comparisons with the results given here.

In the case of the first-order susceptibility $\underline{\underline{\chi}}^{(1)}$, comparison of the different local-field models (namely the rigorous local-field theory with the point-dipole approximation, the rigorous local-field theory with six submolecules and the anisotropic Lorentz field factor approach) revealed no prominent differences, although the rigorous local-field theories generally give better agreement with the available experimental data. However, for the third-order susceptibility $\underline{\underline{\underline{\underline{\chi}}}}^{(3)}$, the Lorentz field factor approximation predicts considerably different results compared to the rigorous local-field models, namely a different ordering of magnitude of the diagonal components, which should be detectable experimentally. The differences between the six-submolecule treatment and the point–dipole model in the rigorous local field theory are rather small. This is not unexpected as benzene is a rather compact molecule in comparison with the intermolecular distances in the crystal and may therefore be well described by the point–dipole model, as argued by Bounds and Munn [5].

Various factors can affect the calculation of the macroscopic optical response of a molecular crystal, even if the local fields are treated rigorously. One factor is a change in the molecular geometry in the crystal environment, but as already noted, we can ignore this factor since experiment shows that any such geometry change is negligible for benzene. Another factor is the effect of the surrounding molecules on the effective molecular response in the crystal environment. The electric field in the crystal caused by the permanent charge distribution of the molecules means that the molecular response required is that at this permanent field rather than at zero field [3], while orbital confinement or valence compression in the crystal means that the electron density cannot distort so freely in an applied electric field because it is restricted by the surrounding molecules all trying to do the same. Since benzene is nonpolar and relatively compact, this factor has been ignored here. The good agreement found with experiment thus confirms that the interactions between benzene molecules in the crystal are rather weak. Considerations similar to these have been used to rationalize the second-harmonic generation observed from crystalline thin films of fullerene, C_{60}, which adopts a centrosymmetric crystal structure; although the centrosymmetry is broken at the surface, the mechanism by which this induces second-harmonic generation relies on the interactions between the molecules and is extremely weak because of the near-spherical molecular symmetry [27]. Hence surface second-harmonic generation in the benzene crystal will presumably also be very weak, although benzene lacks the special features that help to make the bulk magnetic dipole second-harmonic generation so strong in crystalline C_{60}.

Acknowledgement. We acknowledge financial support from the European Commission in the form of a TMR Network Grant (Contract No. ERBFMRXCT960047).

References

1. Janssen RHC, Theodorou DN, Raptis S, Papadopoulos MG, J Chem Phys (submitted)
2. Hurst M, Munn RW (1983) J Mol Electron 2: 35
3. Hurst M, Munn RW (1983) J Mol Electron 2: 43
4. Cummins PG, Dunmur DA, Munn RW, Newham RJ (1976) Acta Crystallogr Sect A 32: 847
5. Bounds PJ, Munn RW (1981) Chem Phys 59: 47
6. Munn RW, Luty T (1983) Chem Phys 81: 41
7. Chemla DS, Oudar JL, Jerphagnon J (1975) Phys Rev B 12: 4534; Zyss J, Oudar JL (1982) Phys Rev A 26: 2028
8. Meyling JH Bounds PJ Munn RW (1977) Chem Phys Lett 51: 234
9. Frisch MJ, Trucks GW, Schlegel HB, Gill PMW, Johnson BG, Robb MA, Cheeseman JR, Keith T, Petersson GA, Montgomery JA, Raghavachari K, Al-Laham MA, Zakrzewski VG, Ortiz JV, Foresman, JB.; Cioslowski J, Stefanov BB, Nanayakkara A, Challacombe M, Peng CY, Ayala PY, Chen W, Wong MW, Andres JL, Replogle ES Gomperts R, Martin, RL, Fox DJ, Binkley JS, Defrees DJ, Baker J, Stewart JP, Head-Gordon M, Gonzalez C, Pople JA (1995) Gaussian 94, revision D.4 Gaussian, Pittsburgh Pa
10. Schmidt MW Baldridge, KK Boatz JA, Elbert ST Gordon MS, Jensen JH, Koseki S, Matsunaga N, Nguyen KA, Su SJ Windus TL Dupuis M Montgomery JA (1993) J Comput Chem 14: 1347
11. Sadlej AJ (1988) Coll Cz Chem Commun 53: 1995

12. Lazzeretti P, Malagoli M, Zanasi R (1990) Chem Phys Lett 167: 101
13. Perrin E, Prasad PN, Mougenot P, Dupuis M (1989) J Chem Phys 91: 4728
14. Adant C, Brédas J-L, Dupuis M (1997) J Phys Chem A 101: 3025
15. Hellwege KH (Editor–in–chief) (1976) Numerical data and functional relationships in science and technology. Landolt–Börnstein, New Series, Group II: Atomic and molecular physics, vol 7. Springer, Berlin Heidelberg New York
16. Cox EG, Cruickshank DWJ, Smith JA (1958) Proc R Soc London Ser A 247: 1
17. Hochstrasser RM, Meredith GR, Trommsdorff HP (1980) J Chem Phys 73: 1009
18. Sekino H, Bartlett RJ (1993) J Chem Phys 98: 3022
19. Rice JE, Handy NC (1992) Int J Quantum Chem 43: 91
20. Rice JE (1992) J Chem Phys 96: 7580
21. Stähelin M, Moylan CR, Burland DM, Willets A, Rice JE (1993) J Chem Phys 98: 5595
22. Rohleder JW, Munn RW (1992) Magnetism and optics of molecular crystals. Wiley Chichester, p 113
23. Adant C, Dupuis M, Brédas J-L (1995) Int J Quantum Chem, Symp 29: 497
24. Zyss J, Chemla DS (1987): In Chemla DS, Zyas J (eds) Nonlinear optical properties of organic molecules and crystals, vol 1. Academic Press, New York, p 23
25. Levine BF, Bethea CG (1975) J Chem Phys 63, 2666
26. See e.g. Hurst M, Munn RW (1986) J Mol Electron 2: 139; Hurst M, Munn RW (1987) J Mol Electron 3: 75; Hurst M, Munn RW (1989): In Hann RA, Bloor D (eds) Organic materials for non-linear optics Royal Society of Chemistry Special Publication No. 69. Royal Society of Chemistry, London, p 3; Hurst M, Munn RW, Morley JA (1990) J Mol Electron 6: 15; Hurst M, Munn RW (1990): In Aviram A (ed) Molecular electronics – science and technology Engineering Foundation, New York, p 267; Munn RW (1992) Int J Quantum Chem 43: 159; Munn RW, Smith SPB (1992) Adv Mater Opt Electron 1: 65
27. Munn RW, Shuai Z, Brédas J-L (1998) J Chem Phys 108: 5975